Electrochemical/Electrospray Mass Spectrometric Studies of I^- and SCN^- at Gold and Platinum Electrodes: Direct Detection of $(SCN)_3^-$

Tan Guo, Lidong Li, Vince Cammarata,* and Andreas Illies*

Department of Chemistry and Biochemistry, Auburn University, Alabama 36849-5312

Received: June 14, 2004; In Final Form: February 15, 2005

Results on the electrochemistry of I^- and SCN^- at gold and platinum electrodes using an electrochemical cell coupled to an electrospray mass spectrometer are reported. We demonstrate that our apparatus is capable of these very challenging electrochemical/electrospray experiments and that $B(C_6H_5)_4^-$ is a suitable internal standard for negative-ion studies in acetonitrile. With I^- at a platinum electrode, we observe well-behaved oxidation to I_3^-. Experiments on I^- at gold electrodes are more complex, showing AuI_2^- as well as I_3^-. The AuI_2^- mass spectrometric ion intensity varies in a complex way throughout the applied electrochemical voltage range studied; we propose that this variation involves the adsorption of I^- on the gold electrode surface. In experiments on SCN^- from $(C_4H_9)_4NSCN$ at gold electrodes, we observe $Au(SCN)_2^-$. Finally, at platinum electrodes, we directly observe $(SCN)_3^-$, a species analogous to I_3^- and $(CN)_3^-$ that has been previously postulated but unverified. This important finding was confirmed by the isotope pattern and demonstrates the stability of the anion.

Introduction

Several research groups have reported successful coupling of electrochemical methods with electrospray mass spectrometry (EC/ESMS).[1−9] This combination has proven to be effective for investigating electrochemical processes.[10−18] The overriding strength of the method is that it promises the full characterization of the details of electrochemical reactions. A difficulty in implementing EC/ESMS is that the electrochemical cell is operated relative to ground potential while the electrospray tip operates at a high potential (±2.5 to 3.6 kV). In addition, for experiments in organic solvents, it has been reported that tetraalkylammonium salts used as electrolytes can severely attenuate electrospray mass spectrometry (ESMS) signals;[19,20] hence it is often necessary to use low concentrations of supporting electrolyte.

We chose to study the iodide system because it undergoes a well-understood multistep oxidation and iodide absorption onto electrode surfaces.[21,28] Studies have also focused on the electrochemistry of gold and its halide complexes in both aqueous and nonaqueous solutions.[29−35] Metallic gold can be dissolved as gold complexes in acetonitrile with strongly coordinating ligands by chemical or electrochemical oxidation.[36] The stepwise stability constants for AuI and AuI_2^- complexes in acetonitrile determined by Fenske indicate that AuI and AuI_2^- are stable in acetonitrile.[37]

The electrochemistry of SCN^- is important since both the S-terminus and N-terminus have the potential to bind to metal surfaces during electroplating processes.[38,39] The electrochemical oxidation of SCN^- has been studied in both aqueous and nonaqueous solutions at a variety of electrode interfaces.[40−43] The initial oxidation product of SCN^- in nonaqueous solutions such as acetonitrile at platinum electrodes is the SCN• radical.[44−47] This radical reacts with SCN^- to form $(SCN)_2^{\bullet-}$, which undergoes further oxidation to form thiocyanogen, $(SCN)_2$.[48] It has been reported that thiocyanogen can then react further with excess SCN^- to form trithiocyanate, $(SCN)_3^-$, analogous to I_3^- and $(CN)_3^-$.[49,50] An alternate mechanism has also been proposed for the production of trithiocyanate from the disproportionation of $(SCN)_2^{\bullet-}$.[51,52] At elevated temperatures at platinum electrodes, the oxidation in acetonitrile leads to an insoluble film, while below room temperature those reactions are negligible.[53,54] The structure of this material "parathiocyanogen" has recently been elucidated by IR spectroscopy.[55]

Based on spectroscopic evidence, trithiocyanate has been previously proposed as the product of the electrochemical oxidation of SCN^- in acetonitrile.[49] It has also been proposed as the electrochemical product of SCN^- oxidation at Au electrodes in dimethyl sulfoxide,[56] while the product of spectroelectrochemical oxidation of SCN^- at a Au minigrid in acidic aqueous solutions has also been proposed as $(SCN)_3^-$.[51] In mass spectrometric experiments, $(SCN)_3^+$ was invoked as a possible product in the photochemical decomposition of solid-state thiocyanates.[57,58] Finally, Barnett and Stanbury suggest that literature disagreements on the UV spectrum of $(SCN)_2$ are likely to be resolved by invoking the formation of $(SCN)_3^-$. However, there is no direct evidence showing $(SCN)_3^-$.[50]

While $(SCN)_3^-$ has been postulated by some workers, others have suggested the oxidation of SCN^- in acetonitrile at gold electrodes results in metal complexes of SCN^- since anodic dissolution occurs at more negative potentials than thiocyanogen formation. It has been reported that both $Au(SCN)_2^-$ and $Au(SCN)_4^-$ are formed,[59] where $Au(SCN)_4^-$ is thought to be an unstable species in the presence of excess SCN^- yielding $Au(SCN)_2^-$ and $(SCN)_2^{\bullet-}$.[60] Pulse radiolysis studies in solution have indicated that $(SCN)_2^{\bullet-}$ binds to the surface of gold nanoparticles,[60] and oxidizes the surface to $[Au^I(SCN)_2]^-$ and the product dissolves into aqueous solution.

In this paper, we demonstrate an electrochemical cell design and our effort to systematically study the electrochemical oxidation of iodide and thiocyanate at platinum and gold electrodes. We sought to identify the products of the oxidation of I^- and SCN^- at both platinum and gold electrodes. By

10.1021/jp047439o CCC: $30.25
Published on Web 04/05/2005

characterizing the soluble products, we hope to identify the relevant electrochemical processes.

Experimental Section

Chemicals and Solutions. Potassium iodide (KI, 99.0+%), sodium tetraphenylborate ($NaB(C_6H_5)_4$), >99.5%), and tetrabutylammonium thiocyanate ($(C_4H_9)_4NSCN$, 98%) were purchased from Aldrich. Analytical grade acetonitrile (CH_3CN) was obtained from Fisher and was distilled from CaH_2. Ammonium thiocyanate (NH_4SCN, 98%, recrystallized three times from acetonitrile) and potassium chloride (KCl, 99.8%) were also obtained from Fisher. Electrochemical grade potassium hexacyanoferrate(III) ($K_3Fe(CN)_6$ >99%) was from Fluka. All salts were used as received except where indicated. Electrolyte solutions of 0.5 mM KI, NH_4SCN, or $(C_4H_9)_4NSCN$ were prepared in freshly distilled CH_3CN with 0.02 mM $NaB(C_6H_5)_4$ as an internal standard.

Instrumentation. A VG-Trios-2000 quadrupole mass spectrometer with VG electrospray source was used in these experiments. Here we report results on anions; the mass spectra were acquired in negative-ion mode coadding 50 scans at a scan rate of 1 scan/s. The ES tip voltage was −2.89 kV, the source temperature was 60 °C, and the cone voltage was typically 20 V. The simulated isotope pattern was determined using iMass (written by Urs Röthlisberger).

A home-built electrochemical cell was made from a cylindrical Pyrex tube, with the working electrode (a 2 mm round ball at the tip of a wire) at one end and a cupped collection assembly leading to the mass spectrometer at the other end (see Supporting Information). The working electrode, a platinum-mesh counter electrode, an Ag/AgCl reference electrode (connected to the cell through a double salt bridge), and the inlet and outlet silica capillaries were made through Viton O-rings or through Supelco Thermogreen LB-2 septa. The working electrodes were made from gold (99.9999%) or platinum (99.9999%) 1 mm wires. The working electrodes themselves were fabricated by melting an ~2 mm diameter ball in a reducing H_2/O_2 flame at one end of the wire.[61,62] Before use, the electrodes were cleaned by rinsing sequentially with distilled water, hydrofluoric acid 49%, piranha[63] solution, distilled water, HPLC grade methanol and fresh acetonitrile.

A CV-27 potentiostat (Bioanalytical System, Inc.) was used to apply potentials to the electrochemical cell and to record the cell current. All potentials are quoted versus aqueous Ag/AgCl at room temperature and range from 0.0 to 2.0 V. Since the residence time of solutions in the sampling area of the electrochemical cell was about 30 s, the time delay between two consecutive potentials was in excess of 60 s. The entire electrochemical cell was maintained at room temperature. An Epsilon-EC potentiostat (Bioanalytical System, Inc.) was used to obtain conventional cyclic voltammograms for comparison purposes.

A Cole Palmer Series 74900 syringe pump with a flow rate of 1.0 mL/h was used to provide the constant mobile phase and produce the spray. To electrically isolate the electrochemical cell from the electrospray tip potential, the cell was connected to the electrospray probe tip through an 800−850 mm long, 0.1 mm i.d. untreated silica capillary.[64]

Results and Discussion

Experiments on the absolute mass spectrometric ion intensity versus mass and applied electrochemical potential for 0.02 mM $NaB(C_6H_5)_4$ in acetonitrile using both platinum and gold electrodes clearly show that the intensity of the tetraphenylborate anion ($B(C_6H_5)_4^-$) does not change with applied potential (see Supporting Information). These results demonstrate that $B(C_6H_5)_4^-$ is a suitable internal standard for experiments at both platinum and gold electrodes; hence all mass spectra were normalized to the $B(C_6H_5)_4^-$ intensity at *m*/*z* 319. As well as having wide voltage limits, sodium tetraphenylborate also has the advantage of good solubility in acetonitrile. Different concentrations of $NaB(C_6H_5)_4$ were evaluated, and a concentration of 0.02 mM appeared optimal.

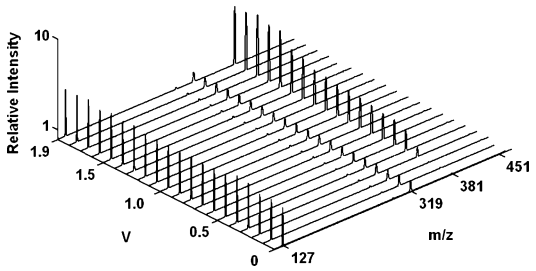

Figure 1. Three-dimensional plot of EC/ESMS ion intensities as a function of potential at a Pt electrode in 0.5 mM KI with 0.02 mM $NaB(C_6H_5)_4$ in CH_3CN. The intensities are all normalized to that of the internal standard, $B(C_6H_5)_4^-$.

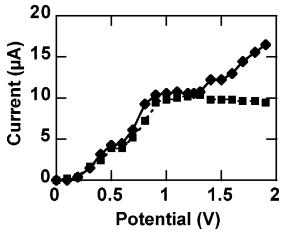

Figure 2. Steady-state current vs potential plot for 0.5 mM KI with 0.02 mM $NaB(C_6H_5)_4$ in CH_3CN at Pt (■) and Au electrodes (◆).

I^- at Pt Electrodes. The cyclic voltammogram of a 0.5 mM KI and 0.02 mM $NaB(C_6H_5)_4$ solution in acetonitrile is shown in the Supporting Information and is consistent with the literature.[21] The voltammogram shows two anodic peaks and one cathodic peak. The anodic peaks correspond to the oxidation of I^- and I_3^-. The cathodic peak is the reduction of I_3^-. Only one cathodic peak corresponding to the reduction of I_3^- is observed in the presence of excess iodide, since most of the I_2 is consumed during the formation of the I_3^- and is not available for the reduction (the equilibrium constant for the formation of I_3^- from I^- and I_2 in acetonitrile is 4×10^6 at 20 °C).[21]

Figure 1 shows the results of a normalized EC/ESMS experiment of the oxidation of KI in acetonitrile at a platinum electrode at potentials from 0.0 to +1.9 V in 0.1 V increments. The mass peak at *m*/*z* 381 corresponds to I_3^- and first appears at +0.3 V; it increases slowly until +1.6 V, beyond which it increases more rapidly and then plateaus. The peaks at *m*/*z* 127 (I^-) and *m*/*z* 319 ($B(C_6H_5)_4^-$) appear relatively constant throughout the voltage range. A small peak at *m*/*z* 293 (difficult to see in the figure) is due to the cluster KI_2^- and is also relatively constant over the entire voltage range. These results clearly demonstrate the formation of I_3^- resulting from the oxidation of I^-.

The steady-state current−voltage curve for I^- at a platinum electrode, collected simultaneously with the spectra, is shown in Figure 2 (squares). The current−potential curve shows two waves at +0.5 and +0.8 V. These are in agreement with the reported current−potential curve of I^-/I_2 in CH_3CN studied using a Pt rotating disk electrode.[21] Figure 2 also shows that the current reaches a mass-transfer-controlled limit starting at 0.9 V. The appearance of I_3^- is confirmed by a color change of

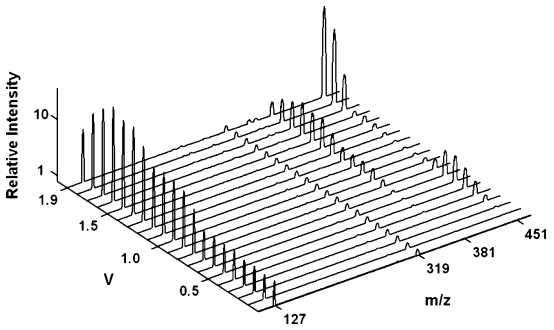

Figure 3. Three-dimensional plot of EC/ESMS ion intensities as a function of potential at a Au electrode of 0.5 mM KI with 0.02 mM $NaB(C_6H_5)_4$ in CH_3CN. The intensities are all normalized to that of the internal standard, $B(C_6H_5)_4^-$.

the solution around the working electrode to the characteristic brown color of I_3^-.

When the absolute intensity of the $B(C_6H_5)_4^-$, I^-, and I_3^- are plotted versus the applied electrochemical potential (not shown), the absolute intensities of $B(C_6H_5)_4^-$ and I^- decrease as the potential is increased and I_3^- is formed. The intensity of the I^- could be interpreted as a decreased I^- concentration resulting from the conversion to I_3^-. However, such an explanation would not account for the steady decrease in the $B(C_6H_5)_4^-$ intensity, which is constant in the control experiment. We suggest that the decrease in I^- and $B(C_6H_5)_4^-$ intensities as the I_3^- intensity increases is due to competition for the overall charge during desolvation in the electrospray process. Hence, the steady decrease in the $B(C_6H_5)_4^-$ intensity and the I^- intensity as I_3^- is formed may be the result of the electrospray ionization process and not an electrochemical phenomenon.

I^- at Au Electrodes. The cyclic voltammogram of KI in CH_3CN at a gold electrode (shown in the Supporting Information) is similar to the voltammogram at platinum electrodes. However, the EC/ESMS spectra of KI at gold electrodes in CH_3CN is quite different. As seen in Figure 3, the mass peak that changes with potential is AuI_2^- *m*/*z* 451. This peak appears at +0.3 V and increases with increasing potential. The peak then starts to decrease at +0.6 V, at which point a peak at *m*/*z* 381 (I_3^-) begins to increase. The intensity of the I_3^- peak reaches a maximum at a potential of +1.7 V, where it starts to gradually decrease. This decrease is also seen in the I^- peak at *m*/*z* 127. Finally, the peak at *m*/*z* 451, corresponding to AuI_2^-, starts to increase again in intensity at $\sim$ +1.7 V. These data indicate that I_3^- is produced at the gold electrode in the potential range of +0.8 to +1.5 V. At less positive potentials, AuI_2^- is formed, and at more positive potentials, AuI_2^- is again formed.

The current−potential curve of I^- at the gold electrode is also shown in Figure 2 (diamonds). The current−potential curves at platinum and gold electrodes are very similar from 0 V to about 1.4 V. However, above 1.4 V the current at the gold electrode begins to rise again; this is in the same region where the AuI_2^- reappears in Figure 3. A plausible interpretation for our observation of AuI_2^- in acetonitrile at low potentials would be the surface oxidation of a gold iodide adlayer to form AuI on the electrode surface. That reaction is followed by the dissolution of the AuI as AuI_2^-, a reaction that is driven by the high stability constant of AuI_2^-. A similar mechanism of gold oxidation with I^- present in water (0.1% acetonitrile) was proposed by Kissner.[36]

The similarity in the current−potential curves at low potential is due to a slow first step, the adsorption of I^-. At a Au electrode, after adsorption of I^-, $Au-I_{(adsorbed)}$ oxidizes to AuI_2^-, while at a Pt electrode the adsorbed I^- oxidizes to I_3^-. The electrode current at the gold electrode shown in Figure 2 does not reach a diffusion-limited region at the most positive potentials. This can be explained by the oxidation of Au to Au^+ that is kinetically limited by the surface area of the electrode and is not solution diffusion limited.

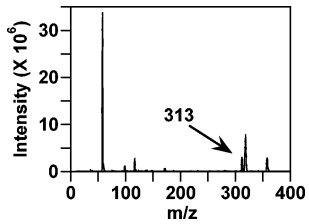

Figure 4. EC/ESMS of a solution of 0.5 mM $(C_4H_9)_4NSCN$ with 0.02 mM $NaB(C_6H_5)_4$ in CH_3CN at a Au electrode. The working electrode is held at +0.8 V.

Although the cyclic voltammograms at Pt and Au are similar (see Supporting Information), the mechanism of oxidation at the two electrodes is quite different as shown by the EC/ESMS three-dimensional plots. These different mechanisms demonstrate the power of the EC/ESMS method in elucidating chemical processes. The experiments on iodide at gold and platinum electrodes may be summarized as follows. With gold electrodes, oxidation of gold in the presence of I^- takes place at low potentials as a surface oxidation process. This is followed by oxidation of I^- from solution at higher potentials that does not involve adsorption. At higher potentials gold is oxidized directly to Au^+, which then complexes free I^-. In contrast, at the platinum electrode, the I^- is adsorbed on the active sites of the platinum electrode,[25] but the oxidation of platinum requires much higher potentials so I^- is oxidized to I_3^-.

SCN^- at Au Electrodes. A representative negative-ion mass spectrum obtained from the EC/ESMS oxidation of SCN^- from $(C_4H_9)_4NSCN$ at a Au working electrode held at 0.8 V is shown in Figure 4. The peak of most interest, that at *m*/*z* 313 corresponding to $Au(SCN)_2^-$, is discussed in detail below. The peaks at *m*/*z* 58 (SCN^-) and *m*/*z* 319 ($B(C_6H_5)_4^-$) correspond to anions directly added to the electrolyte solution: that at *m*/*z* 117 corresponds to $H(SCN)_2^-$, the protonated dimer of thiocyanate, and those at *m*/*z* 99 $[SCN\cdot CH_3CN]^-$, *m*/*z* 358 $[(C_4H_9)_4N(SCN)_2]^-$, and *m*/*z* 658 $[Na(B(C_6H_5)_4)_2]^-$ are a result of cluster formation.

The intensity of $Au(SCN)_2^-$ depends on the electrochemical potential. At potentials below +0.6 V, a small amount of $Au(SCN)_2^-$ is observed. When the potential is increased above +0.6 V, the ion abundance for this species increases and then reaches a steady value at +1.1 V. The mechanism for the formation of $Au(SCN)_2^-$ is not known; however, the appearance of a weak peak at potentials less than +0.6 V followed by an increase in intensity above +0.6 V indicates that $Au(SCN)_2^-$ is possibly formed through two different mechanisms: a surface mechanism and a bulk mechanism (analogous to the two mechanisms for formation of AuI_2^-).

When the absolute ion intensities of $B(C_6H_5)_4^-$, SCN^-, and $Au(SCN)_2^-$ are plotted versus the applied electrochemical potential, the intensities of $B(C_6H_5)_4^-$ and SCN^- decrease as the potential is increased and as the $Au(SCN)_2^-$ increases. This decrease may again be due to an increased competition for the overall charge as the electrospray droplets form ions.

The current−potential diagram for SCN^- at a gold electrode is shown in Figure 5. At potentials below +0.6 V, the current is relatively small but increases rapidly between +0.6 and +1.1 V, where it starts to level off. Both current−potential and ion abundance−potential trends suggest that between +0.6 and

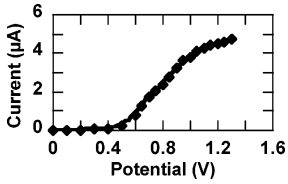

Figure 5. Steady-state current vs potential plot at a Au electrode in 0.5 mM $(C_4H_9)_4NSCN$ with 0.02 mM $NaB(C_6H_5)_4$ in CH_3CN.

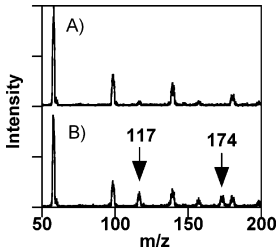

Figure 6. EC/ESMS of a solution of 0.6 mM $(C_4H_9)_4NSCN$ with 0.02 mM $NaB(C_6H_5)_4$ in CH_3CN at a Pt electrode. The working electrode is held at (A) +0.8 V and (B) +1.7 V.

+1.1 V gold can be oxidized and complexed with SCN^- ion. Above +1.1 V, the reaction appears mass transfer limited, most likely by SCN^- transport to the surface.

We also analyzed solutions of NH_4SCN under oxidative conditions at gold electrodes. While the cation might not be expected to affect the electrochemical oxidation of SCN^-, the results were somewhat intriguing. At low potentials the mass spectrum was identical to that of the $(C_4H_9)_4NSCN$ solutions. However, at potentials above +0.3 V, two new species were observed. These new species, at *m*/*z* 249 and 281, correspond to $Au(CN)_2^-$ and $Au(SCN)(CN)^-$, respectively. These peaks corresponding to $Au(CN)_2^-$ and $Au(SCN)(CN)^-$ suggest that the solutions of NH_4SCN may contain CN^- impurities, that the solutions are unstable forming free CN^-, or that the oxidation of SCN^- in the presence of NH_4^+ (NH_3, H^+) results in the cleavage of the S−C bond. Attempts to remove impurities by successive recrystallization did not decrease the intensities of the CN^--containing species. Whatever the source of CN^-, the formation constant for $Au(CN)_2^-$ is greater than that for $Au(SCN)_2^-$; hence, the equilibrium potential is shifted to more negative values. As with the $(C_4H_9)_4NSCN$ experiments, when the electrode potential was greater than +0.6 V, the peak attributed to $Au(SCN)_2^-$ at *m*/*z* 313 was observed.

SCN^- at Pt Electrodes. Solutions of $(C_4H_9)_4NSCN$ at a Pt electrode using the EC/ESMS method were also studied. Figure 6 shows negative-ion mass spectra of a 0.6 mM $(C_4H_9)_4NSCN$ solution with applied potentials of +0.8 V (Figure 6A) and +1.7 V (Figure 6B). Similar to experiments at the gold electrode, anions in the solution (SCN^- *m*/*z* 58 and $B(C_6H_5)_4^-$ *m*/*z* 319) dominate the spectra. Also seen in the spectra are peaks corresponding to the following clusters: $[SCN{\cdot}CH_3CN]^-$, $[SCN{\cdot}(CH_3CN)_2]^-$, $[SCN{\cdot}(CH_3CN)_3]^-$, $[(C_4H_9)_4N(SCN)_2]^-$, and $[(C_4H_9)_4N{\cdot}SCN{\cdot}B(C_6H_5)_4{\cdot}CH_3CN]^-$. The peak corresponding to the proton-bound dimer ($H(SCN)_2^-$) at *m*/*z* 117 shows an increase in intensity with applied potential. This peak is weak below +1.0 V and begins to increase in intensity above +1.0 V; the intensity of this peak plateaus at ~ +1.5 V.

With cell potentials above +1.0 V, an interesting new peak at *m*/*z* 174 appears in the mass spectra. We assign this peak to $(SCN)_3^-$, a species analogous to I_3^- and $(CN)_3^-$.[49,50] As shown in Figure 7, the relative intensity of the *m*/*z* 174 peak (normalized to that of $B(C_6H_5)_4^-$) increases with applied voltage and then plateaus at +1.4 V. To further validate that the peak

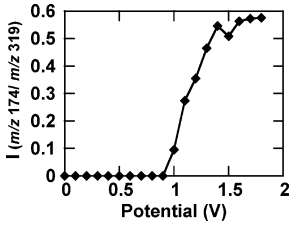

Figure 7. Ratio of mass spectra peak intensities of *m*/*z* 174 to *m*/*z* 319 as a function of working electrode potential. All other conditions as in Figure 6.

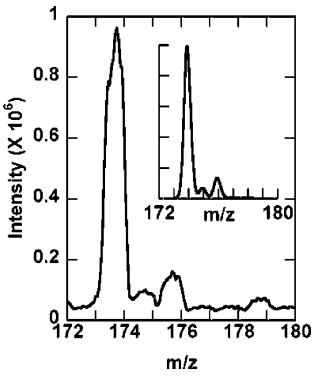

Figure 8. EC/ESMS as in Figure 6 acquiring data between *m*/*z* 172 and 180. The inset shows the calculated isotope pattern at the experimental mass resolution.

at 174 is $(SCN)_3^-$, we recorded and simulated the isotope pattern of $(SCN)_3^-$. Figure 8 shows the expanded mass spectrum of the 174 peak with the inset being the simulated mass spectrum using the natural isotopic distributions. Experimentally, the $(M + 1)^-$ and $(M + 2)^-$ peaks are 6.8% and 13.2% of the base peak while the calculated values are 6.6% and 13.2%, respectively. Thus, the isotope pattern matches that of $(SCN)_3^-$.

In a few experiments at Pt electrodes, a peak at *m*/*z* 311, consistent with $Pt(SCN)_2^-$, was observed at the highest potentials (+2.0 V); however, this peak was not observed in all experiments and efforts at increasing reproducibility were not successful. It is possible that the thickness of the Pt oxide layer formed during the cleaning process has an effect on this reaction, hence its irreproducibility. Nonetheless, it is observed only at the highest potentials (+2.0 V), at potentials more positive than those for the other observed reactions.

The formation of $(SCN)_3^-$ at Pt electrodes but not at Au electrodes throws into doubt spectroelectrochemical experiments at a Au minigrid electrode.[51,52] It also suggests that $Au(SCN)_4^-$ is not an oxidation product in CH_3CN as proposed by Martins et al.[59] ESMS experiments with an authentic sample of $NH_4Au(SCN)_4$ show the complexes $Au(SCN)_4^-$, $Au(CN)(SCN)_3^-$, $Au(SCN)_2^-$, and $Au(CN)(SCN)^-$ are generated. However, in our EC/ESMS experiments only $Au(SCN)_2^-$, $Au(CN)_2^-$, and $Au(CN)(SCN)^-$ are observed. Since we do not observe $Au(SCN)_4^-$ and $Au(CN)(SCN)_3^-$ in our experiments, we conclude that $Au(SCN)_4^-$ is not an oxidation product at Au electrodes. The original spectrochemical work of Cauquis and Pierre,[49] though, used a Pt electrode to perform the electrolysis and we believe this work to be valid. Thus, our work is the first to conclusively demonstrate the electrochemical generation of $(SCN)_3^-$.

Conclusions

The experimental results presented in this paper very clearly demonstrate the power of coupling electrochemical experiments to mass spectrometry. These challenging experiments can

provide a wealth of detailed information on electrochemical processes. We demonstrate that $B(C_6H_5)_4^-$ is a suitable internal standard for negative-ion electrochemical/electrospray mass spectrometric studies in acetonitrile.

Experiments on I^- at a platinum electrode resulted in well-behaved oxidation to I_3^-. With I^- at gold electrodes we observed AuI_2^- as well as I_3^-. The AuI_2^- mass spectrometric ion intensity varies in a nonlinear way throughout the applied electrochemical voltage range studied. We suggest that this variation results from the competition between I^- adsorbed on the gold electrode surface and I^- in solution.

In experiments on SCN^- from $(C_4H_9)_4NSCN$ at gold electrodes, we observe $Au(SCN)_2^-$. When NH_4SCN was used as the source for SCN^- at gold electrodes, we observe $Au(CN)_2^-$ and $Au(CN)(SCN)^-$. This result suggests that NH_4SCN is unstable in acetonitrile and forms CN^- or that the oxidation of SCN^- in the presence of NH_4^+ (NH_3, H^+) results in the cleavage of the S−C bond with formation of CN^-. The direct observation of $(SCN)_3^-$ from $(C_4H_9)_4NSCN$ at platinum electrodes confirms the stability of a previously proposed, but unverified species.

All of the above results demonstrate the power of this experimental method for detection of electrochemically produced species as well as for the elucidation of electrochemical mechanisms.

Acknowledgment. The authors acknowledge the Auburn University Office of the Vice President for Research and the Auburn University Department of Chemistry and Biochemistry for their support.

Supporting Information Available: Electrochemical cell and setup, 3-D plots of the internal standard and the oxidation of SCN^-, and CVs of I^-. This material is available free of charge via the Internet at http://pubs.acs.org.

References and Notes

(1) Pretty, J. R.; Duckworth, D. C.; Van Berkel, G. J. *Anal. Chem.* **1997**, *69*, 3544.
(2) Pretty, J. R.; Deng, H.; Goeringer, D. E.; Van Berkel, G. J. *Anal. Chem.* **2000**, *72*, 2066.
(3) Deng, H.; Van Berkel, G. J. *Anal. Chem.* **1999**, *71*, 4284.
(4) Van Berkel, G. J.; Asano, K. G.; Kertesz, V. *Anal. Chem.* **2002**, *74*, 5047.
(5) Deng, H.; Van Berkel, G. J. *Electroanalysis* **1999**, *11*, 857.
(6) Zhou, F.; Van Berkel, G. J. *Anal. Chem.* **1995**, *67*, 3643.
(7) Van Berkel, G. J.; Zhou, F. *Anal. Chem.* **1995**, *67*, 2916.
(8) Zhang, T.; Palii, S. P.; Eyler, J. R.; Brajter-Toth, A. *Anal. Chem.* **2002**, *74*, 1097.
(9) Zhang, T.; Brajter-Toth, A. *Anal. Chem.* **2000**, *72*, 2533.
(10) Regino, M. C. S.; Weston, C.; Brajter-Toth, A. *Anal. Chim. Acta* **1998**, *369*, 253.
(11) Volk, K. J.; Yost, R. A.; Brajter-Toth, A. *J. Electrochem. Soc.* **1990**, *137*, 1764.
(12) Volk, K. J.; Yost, R. A.; Brajter-Toth, A. *Anal. Chem.* **1992**, *64*, 21A.
(13) Regino, M. C. S.; Brajter-Toth, A. *Electroanalysis* **1999**, *11*, 374.
(14) Regino, M. C. S.; Brajter-Toth, A. *Anal. Chem.* **1997**, *69*, 5067.
(15) Hambitzer, G.; Heitbaum, J.; Stassen, I. *Anal. Chem.* **1998**, *70*, 838.
(16) Modestov, A. D.; Gun, J.; Mudrov, A.; Lev, O. *Electroanalysis* **2004**, *16*, 367.
(17) Van Berkel, G. J.; Asano, K. G.; Granger, M. C. *Anal. Chem.* **2004**, *76*, 1493.
(18) Kertesz, V.; Dunn, N. M.; Van Berkel, G. J. *Electrochim. Acta* **2002**, *47*, 1035.
(19) Tang, L.; Kebarle, P. *Anal. Chem.* **1993**, *65*, 3654.
(20) Lu, W.; Xu, X.; Cole, R. B. *Anal. Chem.* **1997**, *69*, 2478.
(21) Macagno, V. A.; Giordano, M. C.; Arvía, A. J. *Electrochim. Acta* **1969**, *14*, 335.
(22) Arvía, A. J.; Giordano, M. C.; Podestá, J. *Electrochim. Acta* **1969**, *14*, 389.
(23) Swathirajan, S.; Bruckenstein, S. *J. Electroanal. Chem.* **1983**, *143*, 167.
(24) Iwamoto, R. *Anal. Chem.* **1959**, *31*, 955.
(25) Bagotsky, V. S.; Vassilyev, Y. B.; Weber, J.; Pirtskhalava, J. N. *J. Electroanal. Chem.* **1970**, *27*, 31.
(26) Guidelli, R.; Piccardi, G. *Electrochim. Acta* **1967**, *12*, 1085.
(27) Popov, A. I.; Geske, D. H. *J. Am. Chem. Soc.* **1958**, *80*, 1340.
(28) Svensson, P. H.; Rosdahl, J.; Kloo, L. *Chem.—Eur. J.* **1999**, *5*, 305.
(29) Lane, R. F.; Hubbard, A. T. *J. Phys. Chem.* **1975**, *79*, 808.
(30) Sedlmaier, H. D.; Plieth, W. J. *J. Electroanal. Chem.* **1984**, *180*, 219.
(31) McCarley, R. L.; Bard, A. J. *J. Phys. Chem.* **1991**, *95*, 9618.
(32) Goolsby, A. D.; Sawyer, D. T. *Anal. Chem.* **1979**, *40*, 1978.
(33) Ahrland, S.; Nilsson, K.; Persson, I.; Yuchi, A.; Penner-Hahn, E. J. *Inorg. Chem.* **1989**, *28*, 1833.
(34) Cahan, B. D.; Villullas, H. M.; Yeager, E. B. *J. Electroanal. Chem.* **1991**, *306*, 213.
(35) Wagner, D.; Gerischer, H. *J. Electroanal. Chem.* **1989**, *258*, 127.
(36) Kissner, R. *J. Electroanal. Chem.* **1995**, *385*, 71.
(37) Roulet, R.; Lan Quang, N.; Mason, W. R.; Fenske, G. P., Jr. *Helv. Chim. Acta* **1973**, *56*, 2405.
(38) Schlesinger, M.; Paunovic, M. *Modern Electroplating*, 4th ed.; John Wiley & Sons: New York, 2000.
(39) Corrigan, D. S.; Weaver, M. J. *J. Phys. Chem.* **1986**, *90*, 5300.
(40) Kerstein, H.; Hoffmann, R. *Berichte* **1924**, *57*, 491.
(41) Gaugin, R. *Ann. Chim.* **1949**, *4*, 832.
(42) Songina, O. A.; Pavilova, I. M. *Izv. Vyskikh. Uchebn. Zaved. Khim. I Khim. Teckhnol.* **1962**, *5*, 378.
(43) Nicholson, M. M. *Anal. Chem.* **1959**, *31*, 128.
(44) Martinez, C.; Calandra, A. J.; Arvía, A. J. *Electrochim. Acta* **1972**, *17*, 2153.
(45) Pereiro, R.; Arvía, A. J.; Calandra, A. J. *Electrochim. Acta* **1972**, *17*, 1723.
(46) Tomilov, A. P. *Russ. Chem. Rev.* **1961**, *30*, 639.
(47) Cauquis, G.; Pierre, G. *C. R. Acad. Sci. Paris* **1968**, *266*, 883.
(48) Foley, J. K.; Pons, S.; Smith, J. J. *Langmuir* **1985**, *1*, 697.
(49) Cauquis, G.; Pierre, G. *Bull. Soc. Chim. Fr.* **1972**, 2244.
(50) Barnett, J. J.; Stanbury, D. M. *Inorg. Chem.* **2002**, *41*, 164.
(51) Itabashi, E. *J. Electroanal. Chem.* **1984**, *177*, 311.
(52) Itabashi, E. *Inorg. Chem.* **1985**, *24*, 4024.
(53) Calandra, A. J.; Martins, M. E.; Arvía, A. J. *Electrochim. Acta* **1971**, *16*, 2057.
(54) Arvía, A. J.; Calandra, A. J.; Martins, M. E. *Electrochim. Acta* **1972**, *17*, 741.
(55) Cataldo, F.; Kenheyan, Y. *Polyhedron* **2002**, *21*, 1825.
(56) Martins, M. E.; Castellano, C.; Calandra, A. J.; Arvía, A. J. *J. Electroanal. Chem.* **1978**, *92*, 45.
(57) Eremin, L. P.; Luk'yanova, V. A.; Poleshchuk, O. K.; Dolenko, G. N.; Vitkovskii, V. Y. *Russ. J. Phys. Chem.* **1989**, *63*, 1034.
(58) Since it is not stated in the paper (ref 57) we assume that the reported mass spectra in ref 57 are positive-ion mass spectra; hence we suggest that S_5N^+ is a more likely assignment for the peak at *m*/*z* 174. This is especially true in light of the series of nitrogen-containing peaks for S_4N^+ and S_3N^+.
(59) Martins, M. E.; Castellano, C.; Calandra, A. J.; Arvía, A. J. *J. Electroanal. Chem.* **1977**, *81*, 291.
(60) Dawson, A.; Kamat, P. V. *J. Phys. Chem. B* **2000**, *104*, 11842.
(61) Sawyer, D. T.; Sobkowiak, A.; Roberts, J. L., Jr. *Electrochemistry for Chemists*, 2nd ed.; John Wiley & Sons: New York, 1995.
(62) Hsu, T. *Ultramicroscopy* **1988**, *11*, 167. Feliu, J. M.; Claret, J.; Muller, C.; Vazquez, J. L.; Aldaz, A. *J. Electroanal. Chem.* **1984**, *172*, 383.
(63) Licht, S.; Cammarata, V.; Wrighton, M. S. *J. Phys. Chem.* **1990**, *94*, 6133.
(64) Conduction between the electrochemical cell and the electrospray probe tip through the 800 mm silica capillary is minimal due to the low electrolyte concentrations and nonaqueous solvents used.